Prominence of Pairing in Inclusive $(p, 2p)$ and (p, pn) Cross Sections from Neutron-Rich Nuclei

N. Paul, A. Obertelli, C A Bertulani, A. Corsi, P. Doornenbal, J. l. L Rodriguez-Sanchez, G. Authelet, H. Baba, D. Calvet, F. Chateau, et al.

Prominence of Pairing in Inclusive $(p,2p)$ and (p,pn) Cross Sections from Neutron-Rich Nuclei

N. Paul,[1,2,*] A. Obertelli,[3,1,2] C. A. Bertulani,[4] A. Corsi,[1] P. Doornenbal,[2] J. L. Rodriguez-Sanchez,[1,5] G. Authelet,[1] H. Baba,[2] D. Calvet,[1] F. Château,[1] S. Chen,[6,2] A. Delbart,[1] J.-M. Gheller,[1] A. Giganon,[1] A. Gillibert,[1] T. Isobe,[2] V. Lapoux,[1] M. Matsushita,[7] S. Momiyama,[2,8] T. Motobayashi,[2] M. Niikura,[8] H. Otsu,[2] C. Péron,[1] A. Peyaud,[1] E. C. Pollacco,[1] J.-Y. Roussé,[1] H. Sakurai,[2,8] C. Santamaria,[1,2,9] M. Sasano,[2] Y. Shiga,[10] D. Steppenbeck,[2] S. Takeuchi,[2] R. Taniuchi,[2,8] T. Uesaka,[2] H. Wang,[2] K. Yoneda,[2] T. Ando,[2,8] T. Arici,[5,11] A. Blazhev,[12] F. Browne,[13] A. M. Bruce,[13] R. Carroll,[14] L. X. Chung,[15] M. L. Cortés,[3,5,2] M. Dewald,[12] B. Ding,[16] Zs. Dombradi,[17] F. Flavigny,[18] S. Franchoo,[18] F. Giacoppo,[19] M. Górska,[5] A. Gottardo,[18] K. Hadynska-Klek,[19] Z. Korkulu,[17] S. Koyama,[2,8] Y. Kubota,[2,7] A. Jungclaus,[20] J. Lee,[21] M. Lettmann,[3] B. D. Linh,[15] J. Liu,[21] Z. Liu,[16] C. Lizarazo,[5,3] C. Louchart,[3] R. Lozeva,[22,23] K. Matsui,[2,8] T. Miyazaki,[2,8] K. Moschner,[12] S. Nagamine,[8,2] N. Nakatsuka,[24] C. Nita,[25] S. Nishimura,[2] C. R. Nobs,[13] L. Olivier,[18] S. Ota,[7] Z. Patel,[14] Zs. Podolyák,[14] M. Rudigier,[14] E. Sahin,[19] T. Y. Saito,[8,2] C. Shand,[14] P.-A. Söderström,[2,26] I. G. Stefan,[18] T. Sumikama,[27] D. Suzuki,[18] R. Orlandi,[28] V. Vaquero,[20] Zs. Vajta,[17] V. Werner,[3] K. Wimmer,[8] J. Wu,[2,6] and Z. Xu[21]

[1]*IRFU, CEA, Université Paris–Saclay, F-91191 Gif-sur-Yvette, France*
[2]*RIKEN Nishina Center, 2-1 Hirosawa, Wako, Saitama 351-0198, Japan*
[3]*Institut für Kernphysik, Technische Universität Darmstadt, D-64289 Darmstadt, Germany*
[4]*Department of Physics and Astronomy, Texas A&M University-Commerce, Commerce, Texas 75429-3011, USA*
[5]*GSI Helmholtzzentrum für Schwerionenforschung, GmbH, D-64291 Darmstadt, Germany*
[6]*School of Physics and State Key Laboratory of Nuclear Physics and Technology, Peking University, Beijing 100871, People's Republic of China*
[7]*Center for Nuclear Study, The University of Tokyo, RIKEN campus, Wako, Saitama 351-0198, Japan*
[8]*Department of Physics, The University of Tokyo, 7-3-1 Hongo, Bunkyo, Tokyo 113-0033, Japan*
[9]*Nuclear Science Division, Lawrence Berkeley National Laboratory, Berkeley, California 94720, USA*
[10]*Department of Physics, Rikkyo University, 3-34-1 Nishi-Ikebukuro, Toshima, Tokyo 172-8501, Japan*
[11]*Justus-Liebig-Universität Giessen, D-35392 Giessen, Germany*
[12]*Institut für Kernphysik, Universität zu Köln, D-50937 Köln, Germany*
[13]*School of Computing Engineering and Mathematics, University of Brighton, Brighton, England BN2 4GJ, United Kingdom*
[14]*Department of Physics, University of Surrey, Guildford, England GU2 7XH, United Kingdom*
[15]*Institute for Nuclear Science and Technology, VINATOM, P.O. Box 5T-160, Nghia Do, Hanoi, Vietnam*
[16]*Institute of Modern Physics, Chinese Academy of Sciences, Lanzhou 730000, People's Republic of China*
[17]*MTA Atomki, P.O. Box 51, Debrecen H-4001, Hungary*
[18]*Institut de Physique Nucléaire, CNRS-IN2P3, Université Paris–Sud, Université Paris–Saclay, F-91406 Orsay Cedex, France*
[19]*Department of Physics, University of Oslo, N-0316 Oslo, Norway*
[20]*Instituto de Estructura de la Materia, CSIC, 28006 Madrid, Spain*
[21]*Department of Physics, The University of Hong Kong, Pokfulam, Hong Kong*
[22]*IPHC, CNRS/IN2P3, Université de Strasbourg, F-67037 Strasbourg, France*
[23]*CSNSM, CNRS/IN2P3, Université Paris–Sud, F-91405 Orsay Campus, France*
[24]*Department of Physics, Faculty of Science, Kyoto University, Kyoto 606-8502, Japan*
[25]*Horia Hulubei National Institute of Physics and Nuclear Engineering (IFIN-HH), RO-077125 Bucharest, Romania*
[26]*Extreme Light Infrastructure-Nuclear Physics (ELI-NP), 077125 Bucharest-Măgurele, Romania*
[27]*Department of Physics, Tohoku University, Sendai 980-8578, Japan*
[28]*Advanced Science Research Center, Japan Atomic Energy Agency, Tokai, Ibaraki 319-1195, Japan*

(Received 31 October 2018; published 26 April 2019)

Fifty-five inclusive single nucleon-removal cross sections from medium mass neutron-rich nuclei impinging on a hydrogen target at ~250 MeV/nucleon are measured at the RIKEN Radioactive Isotope Beam Factory. Systematically higher cross sections are found for proton removal from nuclei with an even number of protons as compared to odd-proton number projectiles for a given neutron separation energy. Neutron removal cross sections display no even-odd splitting, contrary to nuclear cascade model

predictions. Both effects are understood through simple considerations of neutron separation energies and bound state level densities originating in pairing correlations in the daughter nuclei. These conclusions are supported by comparison with semimicroscopic model predictions, highlighting the enhanced role of low-lying level densities in nucleon-removal cross sections from loosely bound nuclei.

DOI: 10.1103/PhysRevLett.122.162503

Pairing correlations, which lower the energy of an atomic nucleus by coupling nucleons into spin-zero pairs, play a prominent role in nuclear structure [1,2]. They are responsible, for example, for the odd-even mass and nucleon separation energy staggering along isotopic chains and the reduced level density in the low-energy spectra of even-even nuclei. In the case of even-even neutron-rich nuclei, where the separation energy is very low, the ground state is often the only bound state. In the present Letter, we evidence that pairing correlations significantly drive the systematics of inclusive one-nucleon hydrogen-induced knockout cross sections for neutron-rich nuclei.

Nucleon-removal cross sections result from the interplay between nuclear structure and the reaction mechanism. In particular, nucleon-removal reactions at intermediate energies are used to evidence new structure effects far from stability, such as changes in the nuclear mass surface [3] or neutron skins [4]. Observed odd-even staggering in fragmentation cross sections has been understood as originating from the low particle separation energy and level density of the daughter nucleus [5–7]. One-nucleon knockout reactions are a tool of choice for spectroscopic studies, and exclusive cross sections between individual excited states may characterize the overlap between the initial and final wave functions [8,9]. Despite the pervasiveness of these methods, the relevant quantities that drive single nucleon-removal cross sections are still actively studied [10–15].

Here, we provide 55 new inclusive single nucleon-removal cross sections from medium-mass neutron-rich nuclei. The dataset is remarkable due to its size, the range of masses covered, and the low neutron separation energy (S_n) of produced nuclei from 3 to 8 MeV.

The measurements were performed at the Radioactive Isotope Beam Factory operated by the RIKEN Nishina Center for Accelerator-Based Science and the Center for Nuclear Study of the University of Tokyo. The data were collected in six different spectrometer settings over two experimental campaigns, comprising settings 1–3 and 4–6, respectively. Figure 1 shows the secondary beams exploited for this analysis, which extend over a region heretofore unexplored by single nucleon-removal inclusive cross section studies. A ^{238}U primary beam accelerated to 345 MeV/nucleon impinged upon a 3-mm-thick ^{9}Be production target, creating a cocktail of radioactive isotopes through in-flight fission at the entrance of the BigRIPS spectrometer [16]. The mean primary beam intensity was 12 pnA for settings 1–3 and 30 pnA for settings 4–6. Beam tracking and magnetic rigidity ($B\rho$) were provided by parallel-plate avalanche counters (PPACs) at each focal plane [17], energy loss was measured by ionization chambers [18], and plastic scintillators provided time-of-flight information. The nuclides of interest were selected via the $B\rho$-ΔE-$B\rho$ method and identified via the $B\rho$-ΔE-TOF method in the BigRIPS spectrometer [16]. The radioactive fragments then passed through a 38-mm-diameter cryogenic liquid hydrogen target [19] with 110 μm entrance and 150 μm exit Mylar windows located at the object focal point of the downstream ZeroDegree spectrometer [20]. The target length was 102(1) mm for settings 1–3 and 99(1) mm for settings 4–6. The energy at the entrance of the target was ~250 MeV/nucleon. A cut commensurate with the target diameter was applied to the beam spot image at the entrance of the liquid hydrogen target, as reconstructed with the PPAC detectors. Daughter nuclei were created through one nucleon removal in the target, with an energy loss ranging from 79 to 110 MeV/nucleon. The daughter nuclei were identified via the TOF-$B\rho$-ΔE method in the ZeroDegree spectrometer, which was operated in a large acceptance achromatic mode with a momentum acceptance of $\pm 3\%$. Details about the experimental campaigns can be found in [21–27].

Inclusive cross sections were determined based on events that triggered the beam detector according to

$$\sigma_{\mathrm{inc}} = \frac{N_d}{N_p}\frac{1}{T\eta}(1-\gamma), \tag{1}$$

where N_d/N_p is the ratio of daughter to parent nuclei for a given channel, T is a transmission factor explained below, η is the density of the liquid hydrogen target in atoms per square centimeter, and γ is the percentage contribution of daughter nuclides from the empty target and beam line elements. γ was measured from high statistics channels in empty target runs to be 12(2)% for (p, pn) in settings 1–3,

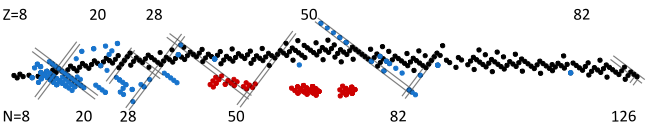

FIG. 1. Chart of the nuclides showing existing data (blue) for inclusive single nucleon-removal cross sections from exotic nuclei near 200 MeV/nucleon (see [12,15,28–55]) and data from this work (red). Parent nuclei are indicated. Stable nuclides are shown in black, and major proton and neutron shell closures are indicated by gray lines.

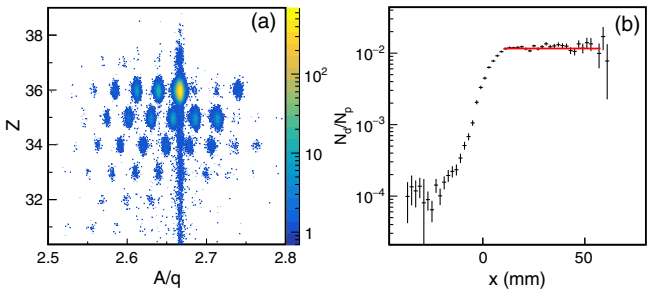

FIG. 2. (a) Particle identification plot of reaction products detected in the ZeroDegree spectrometer for ^{96}Kr incident on target. Z is the proton number of the nucleus, whereas A/q is the mass to charge ratio. The nuclides are assumed to be fully stripped, although charge states are visible for $Z = 36$ beyond $A/q = 2.75$. (b) Ratio of BigRIPS dispersive focal distributions for ^{96}Kr$(p, pn)^{95}$Kr, including the fit used to extract the daughter/parent ratio N_d/N_p. See text for details.

8 (2)% for (p, pn) in settings 4–6, 12 (4) for (p, pn) in settings 1–3, and 8(8)% for $(p, 2p)$ in settings 4–6. The larger contribution in settings 1–3 was due to a difference in the material budget upstream before the target, and the larger uncertainties on the $(p, 2p)$ contribution were due to poorer statistics. As an example of the method to extract N_d/N_p, Fig. 2(a) shows the nuclides transmitted through the ZeroDegree spectrometer for the ^{96}Kr incident on the hydrogen target. The daughter nucleus is selected from this spectrum for the reaction of interest, and the ZeroDegree spectrometer acceptance effects are corrected by examining the part of the incident distribution that yields the daughter. Figure 2(b) shows the ratio between the ^{96}Kr$(p, pn)^{95}$Kr distribution and the ^{96}Kr incident distribution in the BigRIPS dispersive focal plane. The flat region, fit to calculate N_d/N_p, corresponds to daughter nuclei transmitted through the ZeroDegree spectrometer, whereas the sloped regions correspond to $B\rho$ trajectories cut by the spectrometer. N_d/N_p ratios range from 0.00036 to 0.017 for the channels presented in this analysis, with uncertainties ranging from ≤1 to 50% according to the statistics.

The transmission factor accounts for losses from beam line elements and reactions in the thick hydrogen target. It was determined from direct beam runs with both spectrometers magnetically centered on the same nucleus. The same fit method illustrated in Fig. 2(b) was used to correct the transmission for acceptance. The weighted average of both parent and daughter transmissions was utilized if possible; otherwise, the available transmission channel was taken. Transmissions ranged from 40 to 68%, depending on the $B\rho$ relative to the central trajectory, with uncertainties ranging from ≤1 to 50%. For the ^{96}Kr$(p, pn)^{95}$Kr example, the transmission was 58(5)%, which was taken from the statistically weighted average of the parent and daughter transmissions. For empty target runs, the mean transmission through the beam line was 84%.

The target density was calculated via temperature and pressure probes on the cryogenic target. The density was 70.97(3) kg/m^3 for settings 1–3 and 73.22(8) kg/m^3 for settings 4–6, leading to atomic densities of the target of 4.32(4) and 4.33(4) 10^{23} atoms/cm^2, respectively. These values were consistent with the measured energy losses of ions through the target.

Tables of the measured inclusive cross sections are provided in the Supplemental Material [56]. The uncertainties are dominated by statistics, whereas the systematic uncertainty on the particle-identification cuts ranges from 0.3 to 10%, depending on the separation achieved in the ZeroDegree particle identification spectrum. Isomers were present in the beam, which were measured by the EUroball-RIKEN Cluster Array spectrometer [58]. Isomeric contamination was measured for 10 projectiles (^{67}Fe, ^{70}Ni, ^{78}Zn, ^{94,95}Br, ^{95}Kr, $^{96–98}$Rb, and ^{100}Sr) and ranged from 2 to 52% for ^{100}Sr and ^{95}Kr, respectively. This contamination was included as an uncertainty on the number of projectiles in $N_d/N_p = R$, and it was added in quadrature to the uncertainty from the fitting procedure according to $(\delta_R/R)^2 = (\delta_{\rm fit} + R)^2 + {\rm FC}^2$, where $\delta_{\rm fit}$ is the fitting uncertainty and FC is the fractional isomeric contamination.

The measured single proton removal cross sections are shown in Fig. 3(a). Even(odd) proton number projectiles

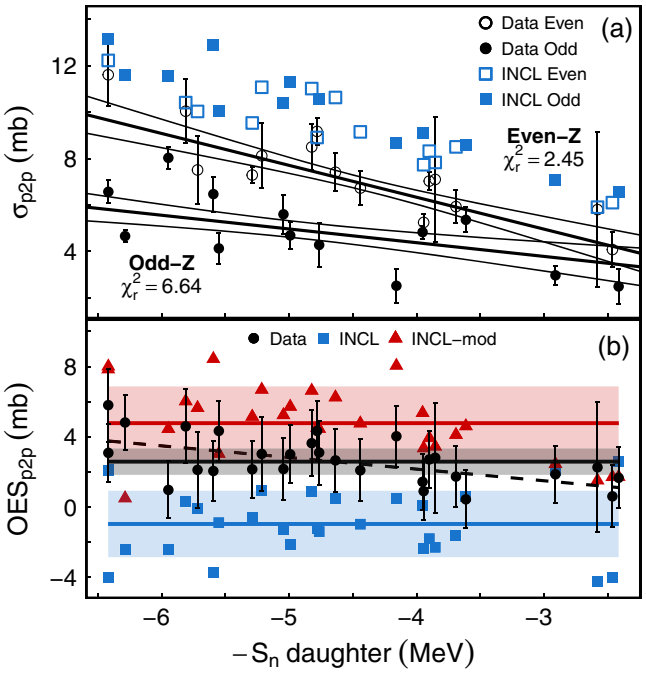

FIG. 3. (a) Inclusive $(p, 2p)$ cross sections measured in this work (black circles) compared with intranuclear cascade (INCL) predictions (blue squares). Even-Z projectiles are shown as open symbols, odd-Z projectiles are shown as filled symbols. (b) Odd-even splitting in the $(p, 2p)$ data compared with INCL (blue squares) and modified INCL (red triangles) calculations. Regressions shown with standard residual uncertainty bands. See text for details.

are shown as open(filled) markers. The $(p,2p)$ cross sections range between 3 and 12 mb, and their systematics manifest two prominent features. The first is a decreasing cross section as S_n decreases, i.e., moving towards the neutron drip line, which is consistent with what was observed, for example, in [14,46]. The second is an odd-even effect wherein even-Z (proton number) projectiles have a cross section consistently higher than the odd-Z projectiles for the same S_n of the daughter nucleus.

Linear regressions of $(p,2p)$ data as a function of $-S_n$ of the daughter nucleus were performed for two hypotheses: (1) an overall linear trend, and (2) separate linear trends for even and odd Z projectiles. These hypotheses were tested by extracting the Akaike information criterion (AIC) for these models, which is a modified χ^2 that penalizes model parameters [59]. The resulting AICs are 235 and 114 for the two respective cases, showing that the separate linear trends for the odd and even Z projectiles are the statistically preferred description of our data. The regressions for case 2 with 68% confidence limits and their associated reduced χ^2 values are shown with the data in Fig. 3(a). The odd-even splitting (OES) may be further quantified by $\mathrm{OES}_{p2p} = [(-1)^Z(\sigma_{\mathrm{even}}(S_n) - \mathrm{fit}_{\mathrm{odd}}(S_n)]$, or vice versa for odd projectiles, where σ indicates the measured cross section and fit indicates the regression. OES_{p2p} is shown in Fig. 3(b), where the uncertainties include the one-sigma experimental error for the measured even(odd)-Z channel and the one-sigma confidence limit from the linear fit of odd(even) Z at the same daughter S_n added in quadrature. A zeroth order regression yields a mean OES_{p2p} of 2.6(3) mb, and thus an odd-even splitting that is consistently larger than zero across the range of S_n values in the data. The measured OES_{p2p} may also be well described by a first order polynomial that decreases with $-S_n$, which is shown as the dashed line in Fig. 3(b). However, as the reduced χ^2 for both zeroth and first order fits are below one, the data do not permit us to reliably confirm such a tendency.

Both the OES_{p2p} and the linear decreasing trend of the cross sections can be related to the strength distribution below S_n in the daughter nuclei. The latter trend may be understood as decreasing S_n, moving towards more neutron-rich nuclei, leads to a reduced strength to $(p,2p)$-populated bound states in the daughter nucleus. As there are fewer states to populate during the $(p,2p)$ reaction, the cross section decreases correspondingly with S_n of the daughter. The odd-even effect may be understood by examining the finer features of the bound state spectrum. In even-Z daughter nuclei (resulting from proton removal from an odd-Z projectile), the pairing interaction leads to a reduced level density, which is visible already in the lowest energy part of the spectrum as a gap between the ground state and the first excited state. This gap may be empirically expressed as the difference of separation energies, $\Delta_p = (-1)^{Z-1}[S_p(Z+1,N) - S_p(Z,N)]$ [2]. When separation energies are low, this effect becomes prominent because Δ_p represents a significant fraction of S_n (~40% for the even-Z daughter nuclides considered here). The above gap is quantitatively valid for spherical nuclei, but it may be distorted in exotic nuclei by correlations such as deformation; see, for example, [60]. Nevertheless, that even-Z nuclei have a lower level density for proton-driven states than odd-Z nuclei remains true [61]. As a quantitative illustration of a specific case, we consider here the strength distribution in the neighboring ^{59}Co and ^{58}Fe stable nuclei after one proton transfer (d, ^{3}He) as published in [62,63]. The ratio of their respective integrated spectroscopic strengths up to 1 MeV is 0.3, with more strength at low energy for ^{59}Co than for ^{58}Fe. This ratio reaches 0.5 when integrated up to 4 MeV, and it reaches 0.7 when integrated up to 6 MeV. We thus attribute the reduction in the cross section for odd-Z projectiles compared to even-Z projectiles to a reduction in the number of bound states having a significant proton-hole nature in the even-Z daughter nuclei. This reduction is thought to stem largely from the impact of pairing on the low-lying level densities. The odd-even effect for these inclusive $(p,2p)$ cross sections in neutron-rich nuclei is evidenced here for the first time.

Although the OES_{p2p} is consistent with a constant value over the range of explored S_n, our data do not exclude a reduction with $-S_n$. If confirmed, such a dependence could originate in a reduction of pairing with increasing neutron excess, as suggested by mass measurements in nuclei near stability [64] and predicted, for example, by [65,66].

The neutron removal cross sections are shown in Fig. 4(a) as a function of projectile mass. The (p,pn) cross sections do not manifest any obvious dependencies on S_n of the daughter nucleus as observed for the proton removal cross sections, nor A, N, or Z. The typical measured cross sections of ~50 mb are consistent with published values from light C, N, and O [67,68], and from Sn isotopes [15]. Although the neutron removal probability is expected to increase with N along an isotopic chain, S_n decreases with A reducing the number of available bound states in the daughter. We note that no obvious shell effects are visible, although the $N = 50$ shell closure is traversed in this dataset at $A = 80$ (^{80}Zn), suggesting that, in the considered nuclei, the S_n is sufficiently high so that shell effects are significantly integrated out in the inclusive cross sections. This may not always be the case, as observed recently in [55], where the neutron removal cross section from ^{134}Sn was found to be half of that from ^{133}Sn, which was attributed to a 5 MeV difference in S_n of the daughter nuclei.

These data show no odd-even splitting of the cross sections along isotopic chains, as quantified in Fig. 4(b), which shows $\mathrm{OES}_{ppn} = (-1)^N(\sigma_N - \sigma_{N+1})$ as a function of projectile mass. The measured OES_{ppn} is fit with a zeroth order regression, which yields a mean OES_{ppn} of

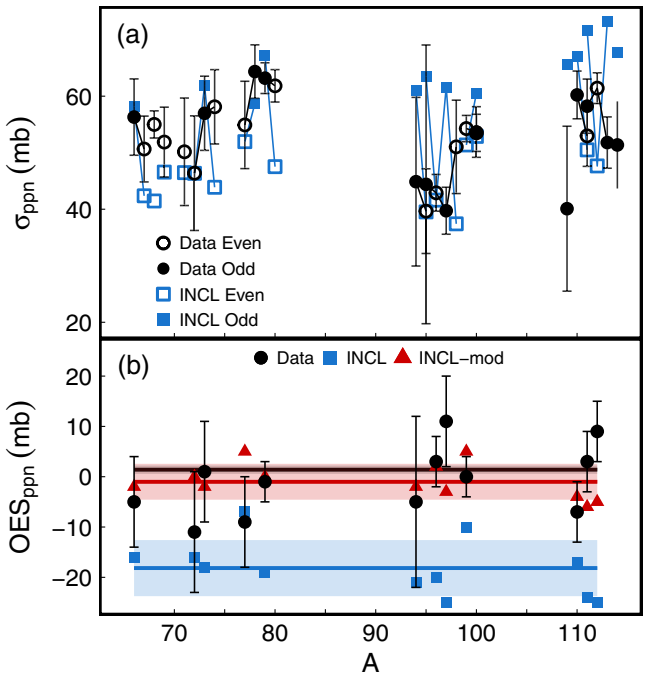

FIG. 4. (a) Inclusive (p, pn) cross sections measured in this work (black circles) compared with INCL predictions (blue squares). Even-N projectiles are shown as open symbols, odd-N projectiles are shown as filled symbols. Adjacent isotopes are connected by lines. (b) Odd-even splitting in the (p, pn) data compared with INCL (blue squares) and modified INCL (red triangles) calculations. Regressions are shown with standard residual uncertainty bands. See text for details.

0(2) mb. This trend is contrary to fragmentation data [5] and predictions from semimicroscopic models (see below). Intuitively, this can be interpreted by the same arguments as in the above discussion of proton removal: the reduced level density in even-N daughter nuclides is compensated by a higher S_n in those same daughters, meaning the total strength to (p, pn)-populated bound states does not change appreciably from neutron-even to neutron-odd daughter nuclei. These combined effects of separation energy and level density yield the lack of OES in the (p, pn) data.

To test our interpretation, the results were compared with semimicroscopic models recently used in the literature to describe inclusive nucleon-removal cross sections. The latest version of the Liège intranuclear cascade model (INCL) [13,69] describes hadron-nucleus reactions as a series of quasiclassical binary collisions in a static potential well, with proton and neutron radial distributions constrained by Hartree-Fock–Bogoliubov (HFB) calculations [70] using the SLy5 interaction [71]. After a certain time scale, the collisions are stopped and the excitation energy of the fragment is calculated based on the kinetic energy of remaining nucleons relative to the ground state of the remnant [72]. The excitation energy is evaporated via γ and particle emission to produce the daughter nucleus [73]. The excitation energy distribution after the fragmentation includes neither structure nor pairing effects, whereas experimental separation energies from the atomic mass evaluation [74] are considered in the evaporation phase. INCL predictions for our measurements are shown in blue in Figs. 3(a) and 4(a), following the same odd-even marker convention as for the data. A slight overestimation is found for proton removal; although, qualitatively, the slope is reproduced. Good average agreement is found for neutron removal, which is consistent with the latest results from [69]. The INCL OES is shown for $(p, 2p)$ and (p, pn) in Figs. 3(b) and 4(b), respectively. INCL fails to reproduce the OES in the $(p, 2p)$ data, where a zeroth order regression yields an OES_{p2p} of -1 mb with a residual standard error (RSE) of 2 mb, as expected due to the lack of a realistic excitation energy spectrum. However, a strong OES is present in the (p, pn) calculations that is not seen in the data, where INCL shows an OES_{ppn} of -18 mb with a RSE of 6 mb. This effect is attributed to the strong effect of pairing on the neutron separation energies, which are included in INCL and lead to higher flux to even-N daughters, which in reality are compensated by the level density effect as described above, with the latter being neglected in the calculations.

To mimic the effect of pairing on inclusive cross sections, a phenomenological correction was made to the INCL excitation energy for odd-$Z(N)$ projectiles for proton(neutron) removal, which was equal to the difference between daughter and projectile separation energies, $E^*_{\mathrm{mod}} = E^*_{\mathrm{INCL}} + (S_{\mathrm{daughter}} - S_{\mathrm{proj}})$, where S is the proton(neutron) separation energy for proton(neutron) removal. This modification shifts the strength to higher excitation energy, reducing flux to the daughter nucleus when the projectile is odd and mimicking the effect of pairing correlations on the cross section. The OES resulting from the modified INCL calculations (INCL-mod) is shown in Figs. 3(b) and 4(b). The modifications generate an OES_{p2p} of 5 mb with a RSE of 2 mb, showing a clear splitting as in the data, although slightly exaggerated. The new predictions reduce the OES_{p2p} to -1 mb with a RSE of 4 mb, further supporting our understanding of the origin of these effects. Quantitatively, the residual between the data and INCL predictions for proton removal is 4(2) mb improving to 2(1) mb for INCL-mod. The neutron removal data residuals are 9(7) mb for both INCL and INCL-mod when compared to our dataset.

The model dependence of these observed trends was tested by comparing the data with fragmentation-evaporation (FE) calculations [4,8,75,76]. In the FE model, collisions occur between nucleons within a sum of cylindrical regions created by the overlapping projectile and target volumes, leaving the fragment with an excitation energy that is released in a second step by evaporation. The excitation energy used for evaporation is determined by the particle-hole energy of the fragment, with single particle densities obtained from HFB calculations with the SLy5

interaction [71]. The global decreasing trend of $(p,2p)$ cross sections with $-S_n$ and a lack of OES_{p2p}, as well as a pronounced OES_{ppn} along isotopic chains, are present in FE calculations as in INCL. FE predictions are given in the Supplemental Material [56].

In summary, we have measured 55 inclusive single nucleon-removal cross sections from neutron-rich medium-mass nuclei impinging on a proton target at energies of ~250 MeV/nucleon. A decreasing trend with $-S_n$ is seen for proton removal, which is consistent with previous works; and a systematic enhancement of the $(p,2p)$ cross section from even-Z projectiles relative to odd-Z projectiles is revealed here for the first time. Meanwhile, no significant enhancement of the neutron removal cross sections is found with added neutron numbers, and no odd-even splitting is seen along isotopic chains, which is contrary to cascade-evaporation model predictions. These general features are understood by simple considerations of the bound state spectrum of the daughter nuclei, which are largely impacted by pairing effects. Inclusive one-nucleon-removal cross sections can probe the nuclear structure at the neutron drip line for nuclei not reachable by spectroscopy. In particular, it is expected from this work that the odd-even splitting in $(p,2p)$ inclusive cross sections may be quenched for very neutron-rich nuclei if pairing correlations decrease close to the drip line.

We express our gratitude to the RIKEN Nishina Center accelerator staff for providing the stable and high-intensity uranium beam and to the BigRIPS team for the smooth operation of the secondary beams. A. O. thanks the European Research Council for its support through ERC Grant No. MINOS-258567, the Japanese Society for the Promotion of Science for the long-term fellowship L-13520, the German DFG SFB Grant No. 1245, and the Alexander von Humboldt Foundation. C. S. acknowledges support by the IPA program at the RIKEN Nishina Center. C. A. B. acknowledges support by U.S. Department of Energy Grant No. DE-FG02-08ER41533 and U.S. National Science Foundation Grant No. 1415656. J. L. R.-S. acknowledges support by the Regional Government of Galicia under the program of postdoctoral fellowships. K. M. acknowledges support from German BMBF Grant No. 05P15PKFNA. M. L. C., M. L., and V. W. acknowledge support from German BMBF Grants No. 05P12RDFN8, No. 05P15RDFN1, and No. 05P12RDFN8, as well as DFG Grant No. SFB 1245. L. X. C. and B. D. L. are supported by the Vietnam MOST through Physics Development Program Grant No. ĐTĐLCN.25/18 and acknowledge the Radioactive Isotope Physics Laboratory of the RIKEN Nishina Center for supporting their stay during the experiment. A. J. and V. V. acknowledge support from the Spanish Ministerio de Economía y Competitividad under Contract No. FPA2014-57196-C5-4-P. U.K. participants acknowledge support from the Science and Technology Facilities Council (STFC). Collaborators from I. M. P. were supported by the National Natural Science Foundation of China and the Chinese Academy of Sciences.

*nancy.paul@lkb.upmc.fr
Present address: Laboratoire Kastler Brossel, Sorbonne Université, CNRS, ENS-PSL Research University, Collège de France, Case 74, 4, place Jussieu, F-75005 Paris, France.

[1] R. A. Broglia, O. Hansen, and C. Riedel, *Advances in Nuclear Physics* (Springer, Boston, 1973), pp. 287–457.
[2] A. Bohr and B. R. Mottelson, *Nuclear Structure* (Benjamin, New York, 1998).
[3] O. B. Tarasov, D. J. Morrissey, A. M. Amthor, T. Baumann, D. Bazin, A. Gade, T. N. Ginter, M. Hausmann, N. Inabe, T. Kubo, A. Nettleton, J. Pereira, M. Portillo, B. M. Sherrill, A. Stolz, and M. Thoennessen, Phys. Rev. Lett. **102**, 142501 (2009).
[4] T. Aumann, C. A. Bertulani, F. Schindler, and S. Typel, Phys. Rev. Lett. **119**, 262501 (2017).
[5] M. Ricciardi, A. Ignatyuk, A. Kelić, P. Napolitani, F. Rejmund, K.-H. Schmidt, and O. Yordanov, Nucl. Phys. **A733**, 299 (2004).
[6] P. Napolitani, F. Rejmund, L. Tassan-Got, M. V. Ricciardi, A. Kelić, K.-H. Schmidt, O. Yordanov, A. Ignatyuk, and C. Villagrasa-Canton, Int. J. Mod. Phys. E **13**, 333 (2004).
[7] B. Mei, X. L. Tu, and M. Wang, Phys. Rev. C **97**, 044619 (2018).
[8] C. A. Bertulani and P. Danielewicz, *Introduction to Nuclear Reactions* (Institute of Physics, Bristol and Philadelphia, 2004), p. 515.
[9] T. Wakasa, K. Ogata, and T. Noro, Prog. Part. Nucl. Phys. **96**, 32 (2017).
[10] A. Gade, D. Bazin, B. A. Brown, C. M. Campbell, J. A. Church, D. C. Dinca, J. Enders, T. Glasmacher, P. G. Hansen, Z. Hu, K. W. Kemper, W. F. Mueller, H. Olliver, B. C. Perry, L. A. Riley, B. T. Roeder, B. M. Sherrill, J. R. Terry, J. A. Tostevin, and K. L. Yurkewicz, Phys. Rev. C **69**, 034311 (2004).
[11] J. A. Tostevin and A. Gade, Phys. Rev. C **90**, 057602 (2014).
[12] L. Audirac *et al.*, Phys. Rev. C **88**, 041602(R) (2013).
[13] D. Mancusi, A. Boudard, J. Carbonell, J. Cugnon, J.-C. David, and S. Leray, Phys. Rev. C **91**, 034602 (2015).
[14] J. Benlliure, EPJ Web Conf. **88**, 00028 (2015).
[15] J. L. Rodríguez-Sánchez *et al.*, Phys. Rev. C **96**, 034303 (2017).
[16] N. Fukuda, T. Kubo, T. Ohnishi, N. Inabe, H. Takeda, D. Kameda, and H. Suzuki, Nucl. Instrum. Methods Phys. Res., Sect. B **317**, 323 (2013).
[17] H. Kumagai, T. Ohnishi, N. Fukuda, H. Takeda, D. Kameda, N. Inabe, K. Yoshida, and T. Kubo, Nucl. Instrum. Methods Phys. Res., Sect. B **317**, 717 (2013).
[18] K. Kimura, T. Izumikawa, R. Koyama, T. Ohnishi, T. Ohtsubo, A. Ozawa, W. Shinozaki, T. Suzuki, M. Takahashi, I. Tanihata, T. Yamaguchi, and Y. Yamaguchi, Nucl. Instrum. Methods Phys. Res., Sect. A **538**, 608 (2005).
[19] A. Obertelli *et al.*, Eur. Phys. J. A **50**, 8 (2014).

[20] T. Kubo, D. Kameda, H. Suzuki, N. Fukuda, H. Takeda, Y. Yanagisawa, M. Ohtake, K. Kusaka, K. Yoshida, N. Inabe, T. Ohnishi, A. Yoshida, K. Tanaka, and Y. Mizoi, Prog. Theor. Exp. Phys. (**2012**) 3C003.
[21] C. Santamaria *et al.*, Phys. Rev. Lett. **115**, 192501 (2015).
[22] N. Paul *et al.*, Phys. Rev. Lett. **118**, 032501 (2017).
[23] F. Flavigny *et al.*, Phys. Rev. Lett. **118**, 242501 (2017).
[24] M. Lettmann *et al.*, Phys. Rev. C **96**, 011301 (2017).
[25] S. Chen *et al.*, Phys. Rev. C **95**, 041302(R) (2017).
[26] L. Olivier *et al.*, Phys. Rev. Lett. **119**, 192501 (2017).
[27] C. Shand *et al.*, Phys. Lett. B **773**, 492 (2017).
[28] E. Sauvan, F. Carstoiu, N. A. Orr, J. S. Winfield, M. Freer, J. C. Angélique, W. N. Catford, N. M. Clarke, M. MacCormick, N. Curtis, S. Grévy, C. Le Brun, M. Lewitowicz, E. Liégard, F. M. Marqués, P. Roussel-Chomaz, M.-G. Saint Laurent, and M. Shawcross, Phys. Rev. C **69**, 044603 (2004).
[29] K. L. Yurkewicz, D. Bazin, B. A. Brown, J. Enders, A. Gade, T. Glasmacher, P. G. Hansen, V. Maddalena, A. Navin, B. M. Sherrill, and J. A. Tostevin, Phys. Rev. C **74**, 024304 (2006).
[30] A. Gade, P. Adrich, D. Bazin, M. D. Bowen, B. A. Brown, C. M. Campbell, J. M. Cook, T. Glasmacher, P. G. Hansen, K. Hosier, S. McDaniel, D. Mcglinchery, A. Obertelli, K. Siwek, L. A. Riley, J. A. Tostevin, and D. Weisshaar, Phys. Rev. C **77**, 044306 (2008).
[31] C. A. Diget, P. Adrich, D. Bazin, M. D. Bowen, B. A. Brown, C. M. Campbell, J. M. Cook, A. Gade, T. Glasmacher, K. Hosier, S. McDaniel, D. McGlinchery, A. Obertelli, L. A. Riley, K. Siwek, J. R. Terry, J. A. Tostevin, and D. Weisshaar, Phys. Rev. C **77**, 064309 (2008).
[32] F. Flavigny, A. Obertelli, A. Bonaccorso, G. F. Grinyer, C. Louchart, L. Nalpas, and A. Signoracci, Phys. Rev. Lett. **108**, 252501 (2012).
[33] R. Shane, R. J. Charity, L. G. Sobotka, D. Bazin, B. A. Brown, A. Gade, G. F. Grinyer, S. McDaniel, A. Ratkiewicz, D. Weisshaar, A. Bonaccorso, and J. A. Tostevin, Phys. Rev. C **85**, 064612 (2012).
[34] N. Kobayashi *et al.*, Phys. Rev. C **86**, 054604 (2012).
[35] G. F. Grinyer, D. Bazin, A. Gade, J. A. Tostevin, P. Adrich, M. D. Bowen, B. A. Brown, C. M. Campbell, J. M. Cook, T. Glasmacher, S. McDaniel, A. Obertelli, K. Siwek, J. R. Terry, D. Weisshaar, and R. B. Wiringa, Phys. Rev. C **86**, 024315 (2012).
[36] S. R. Stroberg, A. Gade, J. A. Tostevin, V. M. Bader, T. Baugher, D. Bazin, J. S. Berryman, B. A. Brown, C. M. Campbell, K. W. Kemper, C. Langer, E. Lunderberg, A. Lemasson, S. Noji, F. Recchia, C. Walz, D. Weisshaar, and S. J. Williams, Phys. Rev. C **90**, 034301 (2014).
[37] Z. Y. Sun, D. Yan, S. T. Wang, S. W. Tang, X. H. Zhang, Y. H. Yu, K. Yue, L. X. Liu, Y. Zhou, F. Fang, J. D. Chen, J. L. Chen, P. Ma, and C. G. Lu, Phys. Rev. C **90**, 037601 (2014).
[38] R. Thies *et al.*, Phys. Rev. C **93**, 054601 (2016).
[39] L. Atar *et al.*, Phys. Rev. Lett. **120**, 052501 (2018).
[40] S. Kawase *et al.*, Prog. Theor. Exp. Phys. (**2018**) 021D01.
[41] N. N. G. Zaitseva, M. Y. M. Y. Kuznetsova, M. N. Buk, and V. Khalkin, J. Exp. Theor. Phys. **16**, 1180 (1963).
[42] P. P. Strohal and A. A. Caretto, Phys. Rev. **121**, 1815 (1961).
[43] D. L. Morrison and A. A. Caretto, Phys. Rev. **127**, 1731 (1962).
[44] W. R. Ware and E. O. Wiig, Phys. Rev. **122**, 1837 (1961).
[45] D. L. Morrison and A. A. Caretto, Phys. Rev. **133**, B1165 (1964).
[46] R. F. Schall and A. A. Caretto, Phys. Rev. C **2**, 1924 (1970).
[47] J. Enders, T. Baumann, B. A. Brown, N. H. Frank, P. G. Hansen, P. R. Heckman, B. M. Sherrill, A. Stolz, M. Thoennessen, J. A. Tostevin, E. J. Tryggestad, S. Typel, and M. S. Wallace, Phys. Rev. C **67**, 064301 (2003).
[48] G. Cerizza *et al.*, Phys. Rev. C **93**, 021601 (2016).
[49] S. Momiyama *et al.*, Phys. Rev. C **96**, 034328 (2017).
[50] S. Schwertel *et al.*, Eur. Phys. J. A **48**, 191 (2012).
[51] H. Liu *et al.*, Phys. Lett. B **767**, 58 (2017).
[52] T. Nakamura *et al.*, Phys. Rev. Lett. **112**, 142501 (2014).
[53] Z. Elekes *et al.*, Eur. Phys. J. Spec. Top. **150**, 99 (2007).
[54] D. Pérez-Loureiro *et al.*, Phys. Lett. B **703**, 552 (2011).
[55] V. Vaquero *et al.*, Phys. Rev. Lett. **118**, 202502 (2017).
[56] See Supplemental Material at http://link.aps.org/supplemental/10.1103/PhysRevLett.122.162503 for tables of the experimental cross sections and predictions from INCL and Fragmentation-Evaporation models, which includes Ref. [57].
[57] O. Tarasov and D. Bazin, Nucl. Instrum. Methods Phys. Res., Sect. B **266**, 4657 (2008).
[58] P.-A. Söderström *et al.*, Nucl. Instrum. Methods Phys. Res., Sect. B **317**, 649 (2013).
[59] H. Akaike, IEEE Trans. Autom. Control **19**, 716 (1974).
[60] S. Kreim *et al.*, Phys. Rev. C **90**, 024301 (2014).
[61] V. V. Canuto and L. Garcia-Colin, Nucl. Phys. **A61**, 177 (1965).
[62] G. Mairle *et al.*, Nucl. Phys. **A543**, 588 (1992).
[63] M. Niwano, T. Ishimatsu, R. Asano, T. Suehiro, and M. Tanaka, Nucl. Phys. **A377**, 148 (1982).
[64] X. L. Tu, X. G. Zhou, D. J. Vieira, J. M. Wouters, Z. Y. Zhou, H. L. Seifert, and V. G. Lind, Z. Phys. A **337**, 361 (1990).
[65] D. G. Madland and J. Nix, Nucl. Phys. **A476**, 1 (1988).
[66] A. Pastore, J. Margueron, P. Schuck, and X. Viñas, Phys. Rev. C **88**, 034314 (2013).
[67] P. Díaz Fernández *et al.*, Phys. Rev. C **97**, 024311 (2018).
[68] D. Cortina-Gil *et al.*, Eur. Phys. J. A **10**, 49 (2001).
[69] J. L. Rodríguez-Sánchez, J.-C. David, D. Mancusi, A. Boudard, J. Cugnon, and S. Leray, Phys. Rev. C **96**, 054602 (2017).
[70] K. Bennaceur and J. Dobaczewski, Comput. Phys. Commun. **168**, 96 (2005).
[71] E. Chabanat, P. Bonche, P. Haensel, J. Meyer, and R. Schaeffer, Nucl. Phys. **A635**, 231 (1998).
[72] A. Boudard, J. Cugnon, S. Leray, and C. Volant, Phys. Rev. C **66**, 044615 (2002).
[73] A. Kelic, M. V. Ricciardi, and K.-H. Schmidt, in *Proceedings of the Joint ICTP-IAEA Advanced Workshop on Model Codes for Spallation Reactions* (IAEA, Vienna, 2008), pp. 181–221.
[74] M. Wang, G. Audi, F. G. Kondev, W. Huang, S. Naimi, and X. Xu, Chin. Phys. C **41**, 030003 (2017).
[75] J. Hüfner, K. Schäfer, and B. Schürmann, Phys. Rev. C **12**, 1888 (1975).
[76] C. A. Bertulani and C. De Conti, Phys. Rev. C **81**, 064603 (2010).